




Research Article

Scheduling in Wireless Cooperative Localization Networks with Intelligent Eavesdroppers

Ming Liu ¹, Mu Jia ^{1,2} and Tingting Zhang ^{2,3}

¹School of Microelectronics, Shenzhen Institute of Information Technology, Shenzhen, China

²School of Electronic and Information Engineering, Harbin Institute of Technology, Shenzhen, China

³Shenzhen Peng Cheng Laboratory, Shenzhen, China

Correspondence should be addressed to Tingting Zhang; zhangtt@hit.edu.cn

Received 4 August 2022; Revised 25 July 2023; Accepted 22 August 2023; Published 28 September 2023

Academic Editor: Enrico M. Vitucci

Copyright © 2023 Ming Liu et al. This is an open access article distributed under the Creative Commons Attribution License, which permits unrestricted use, distribution, and reproduction in any medium, provided the original work is properly cited.

Location-based service based on wireless cooperative localization networks is becoming ubiquitous nowadays. However, since the fact that most location network nodes are resource-limited, recent investigations focus on the proper network scheduling strategies that can significantly enhance the system performance, including but not limited to localization accuracy and energy efficiency. In addition to the current efficient nondata-aided strategies, we find that some silent nodes, called “eavesdroppers,” can be helpful to the localization task without transmitting any signals. In this paper, we first formulate the eavesdropping scheduling policy in practical *asynchronous* cooperative wireless localization networks. Then, we perform resource optimization in different eavesdropping-based strategies. Both two-slot and multislot strategies are considered, and three types of listening modes are designed from a practical point of view. Numeric results show that, for the scenario with a blocked propagation path, the localization error of networks with dedicated eavesdroppers is only 21% of the conventional networks. Besides, the system with eavesdropping anchors could improve the localization performance by 70%. The result could provide meaningful insights into the practical low-complexity location network deployment and development.

1. Introduction

As the Internet of Everything has become a hot spot in the development of science and technology, the demand for location information is also increasing. Traffic navigation, logistics tracking, indoor monitoring, environmental detection, hazard warning to search and rescue, all these location-based service (LBS) need the support of positioning technology [1–7]. In most complicated environments, where the open sky can not be guaranteed or more accurate location information is required, wireless network localization provides promising alternatives in addition to satellite navigation systems [8, 9].

In typical location-aware networks, the agent whose position remains unknown needs measurements with multiple predeployed anchors. Different measurements, including the time of arrival (TOA), received signal strength intensity, angle of arrival, and their combinations, are usually adopted [10, 11]. TOA-based ranging and localization provide high-

accuracy solutions, but one implicit assumption in this measurement method is that all involved nodes are *clock synchronized* (high-accuracy ranging and localization requires the clock synchronization as nano-second level), which is challenging in practical wireless networks, especially when the number of network nodes is large [12]. Therefore, asynchronous TOA-based solutions, such as the round trip measurements (RTM) and time difference of arrival, are popular in such scenarios [13]. Generally, the asynchronous solutions may degrade in localization accuracy but achieve tradeoffs in system complexity.

Furthermore, ultra-wideband (UWB) technology has gained significant attention in the field of wireless cooperative localization networks [14, 15]. It can transmit low-power, short-duration pulses, which is well-suited for accurate positioning and ranging in wireless localization networks. The wide bandwidth allows for precise TOA measurements, which can further improve the accuracy of localization algorithms. UWB-based systems have shown promising results in various applications,

such as indoor positioning, asset tracking, and wireless sensor networks (WSNs) [16–18].

The accuracy of network localization is largely determined by the accuracy of range measurements and the network topology. Generally, we need to specify the topology of sensor network, and thus, the power for the transmitter needs to improve for a better localization performance, which increases the resource consumption and system complexity, especially for real-world cases (e.g., WSNs). In the face of resource and cost constraints, resource allocation optimization has proven to be an effective solution [19, 20]. In wireless positioning networks, system positioning resources are relatively limited because of hardware constraints. Thus, appropriate resource allocation schemes are required to benefit the service life of the system and increase the positioning accuracy of the system [21, 22]. Based on the background of wireless positioning networks, resources usually refer to power, bandwidth, spectrum, etc. [23–26]. Furthermore, compared with the optimization of one specific resource, joint resource optimization can explore the potential of the localization system as much as possible with constrained resource consumption [27, 28].

In addition, the cooperation idea can also effectively improve the positioning accuracy under the above constraints. Considering that in ubiquitous LBS, when the scale of localization networks increases or the coverage becomes large, some specific agents cannot be detected with limited anchors (in a 2D scenario, a minimum of three anchors is required), especially in complicated environments with several obstacles. Currently, cooperative positioning has been widely used in various networks. Liu et al. [29] and Peng et al. [30] mentioned that cooperative positioning is a promising solution to the problem of vehicle high-precision positioning. In the study of Mendrzik and Bauch [9], researchers introduce a cooperative idea into indoor localization and propose the framework of position-constrained stochastic inference, which can reduce the requirements of agents. Salari et al. [31] proposed to realize cooperative positioning by means of moving anchors, which is verified to be suitable for large-scale WSNs.

However, communication requirements of cooperation increase the system complexity and energy consumption. In order to improve the above problems, a reasonable scheduling strategy is necessary. Considering that the existing allocation algorithms have been developed to optimize throughput and delay instead of navigation performance [32, 33], proposed a framework to construct a distributed optimization scheme for WSNs. In addition, existing researches also illustrate that when the scheduling scheme is adopted properly, some anchors can also realize localization task without transmitting any signals [34–36].

In this study, we introduce eavesdroppers into a *centralized* (a server is assumed to be able to collect all parameters of the network) nondata-aided allocation scheme for asynchronous UWB-based cooperative sensor networks using RTMs. We consider different eavesdropping strategies and perform resource optimization to achieve a better localization accuracy in this proposed networks. Finally, we provide a

simulation of bandwidth allocation for the system and propose a high-precision algorithm to solve the resource allocation problem. Our numerical results demonstrate the value of eavesdropping with the existence of blocked RTMs, which have better performance than conventional wireless localization networks. The main contribution of this article can be summarized as follows:

- (i) The ranging information intensity (RII) of the eavesdropping wireless localization network is derived to calculate the positioning error bound as the performance metric.
- (ii) Different eavesdropping strategies are introduced in the system to enhance the localization accuracy with the existence of blocked RTMs.
- (iii) Agents with eavesdropping functions are discussed to further allocate the power and bandwidth while optimizing the system performance in multitime slots.

2. System Model

2.1. Network Settings and Signal Models. In a conventional localization sensor network, N_b anchor nodes are preposed with known positions while the locations of N_a agents need estimating. Aiming at the practical issue, all network nodes are asynchronous in clocks, implying the ranges between any nodes are able to be obtained with the RTMs. All ranging information (RI) is forwarded to a server where the localization algorithms are carried out. In this work, the data to be processed is relatively small; we can assume that we use a different band or time to send the data back. Even though the data collection is an essential part of the centralized system, it is a secondary aspect beyond this study [37]. The state of anchors and agents can be represented by $\mathcal{N}_a = \{1, 2, \dots, N_a\}$ and $\mathcal{N}_b = \{1, 2, \dots, N_b\}$ separately. Meanwhile, the location of node k is expressed as $\mathbf{p}_k = [x_k, y_k]^T$, $k \in \mathcal{N}_a \cup \mathcal{N}_b$.

The signal which is received by node j and transmitted from node k , experiencing a multipath propagation, is derived as follows (in this paper, we adopt the IEEE 802.15.4a CM1 channel model as the propagation environment [38], since it is a typical scenario for UWB ranging):

$$r_{kj}(t) = \sum_{l=1}^{L_{kj}} \sqrt{\frac{P_k}{d_{kj}^\alpha}} \alpha_{kj}^{(l)} s(t - \tau_{kj}^{(l)}) + z_{kj}(t), \quad t \in [0, T_{ob}), \quad (1)$$

where P_k represents power at transmitter for node k , d_{kj} means the range difference from node k to node j , $s(t)$ is the transmitted signal with normalized power, q represents the path loss factor for the correspond detection, the amplitude after normalization is represented by $\alpha_{kj}^{(l)}$, the l th path delay is represented with $\tau_{kj}^{(l)}$, $z_{kj}(t)$ is the additive white Gaussian noise, and for the wireless link, there are totally L_{kj} multipath components. $[0, T_{ob})$ illustrate the measurement interval.

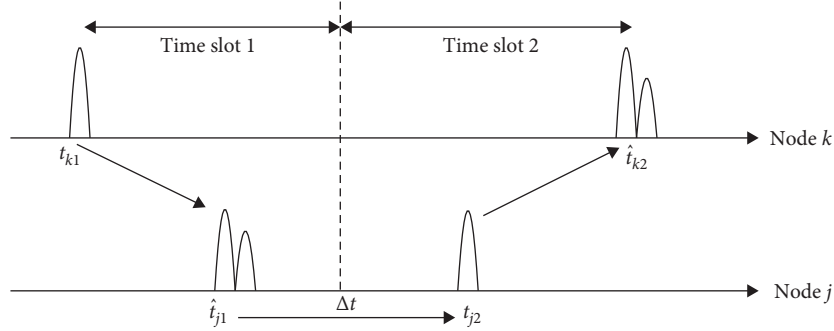


FIGURE 1: Traditional range estimation using round trip measurements.

Because there exist clock offsets among the sensor nodes, we adopt the RTM to derive the distance information. As shown in Figure 1, the estimated RTM can be split into two time slots with two nodes. For the first slot, the observation is originated from agent k , and then the anchor j finishes the RTM with a replied signal in the second time slot. The distance from node k to node j can be derived by the following:

$$\hat{d}_{kj} = \frac{c}{2} [(\hat{t}_{k2} - t_{k1}) - (t_{j2} - \hat{t}_{j1})]. \quad (2)$$

TOA estimated at anchor k and j is represented with \hat{t}_{k2} and \hat{t}_{j1} . In this case, the measured error is obeyed to Gaussian distribution, and the variance is as follows:

$$\sigma_{kj}^2 = \frac{1}{4} (\sigma_{k2}^2 + \sigma_{j1}^2), \quad (3)$$

where the σ_{k2}^2 and σ_{j1}^2 are the variance at time \hat{t}_{k2} and \hat{t}_{j1} , respectively.

2.2. Error Analysis for TOA-Based RTM. In our work, the clock offsets between different nodes are not considered for TOA-based RTMs. We can model the RTMs error as a Gaussian distribution for multipath environments [26]. The RII is used to analyze the localization performance, which is the inverse form of the Cramer–Rao lower bound (CRLB) for localization errors [39]. The RII between anchor k and agent j can be represented as follows:

$$\lambda_{kj} = \xi_{kj} \frac{4P_{k1}\beta_{k1}^2 P_{j2}\beta_{j2}^2}{d_{kj}^2 (P_{k1}\beta_{k1}^2 + P_{j2}\beta_{j2}^2)}, \quad (4)$$

where P_{k1} represents the power of node k used for the transmitting signal in the first time slot of RTM, and β_{k1} is the bandwidth occupied by the signal. P_{j2} represents the power of node j during the second time slot for replied signal, while β_{j2} is the bandwidth occupied by the signal. It is noticeable that if the waveform of the signal is designed properly (e.g., sinc-shaped pulses) with a fixed carrier frequency, the effective bandwidth is able to be equivalent (or approximate) to the practical bandwidth of the signal [27]. The channel coefficient ξ_{kj} is decided by the properties of the channel. For

instance, the overlap factor of transmit path, the normalized direct path (DP) signal amplitude, and the energy of the signal [19, 39]. For simplification and without loss of generality, ξ_{kj} is described as a positive constant to scale the derived RII.

2.3. Position Error Bound. According to Shen et al. [40], the squared position error bound (SPEB), derived from the CRLB, is calculated based on the equivalent Fisher information matrix (EFIM). The SPEB of node k can be defined as follows:

$$\mathbb{E}\{\|\hat{\mathbf{p}}_k - \mathbf{p}_k\|^2\} \geq \mathcal{P}(\mathbf{p}_k) \triangleq \text{tr}\{\mathbf{J}_e^{-1}(\mathbf{p}_k)\}, \quad (5)$$

where $\hat{\mathbf{p}}_k$ means the estimated position of \mathbf{p}_k , $\mathbf{J}_e(\mathbf{p}_k)$ represents the EFIM of node k 's position from observation.

The EFIM of N_a agents for a WSN are able to be represented by a $2N_a \times 2N_a$ matrix. In EFIM, the (i, j) th element is as follows:

$$\mathbf{J}_{ij} = \begin{cases} \mathbf{J}_e^A(\mathbf{p}_i) + \sum_{i \neq j} \mathbf{C}_{i,j} & i = j \\ -\mathbf{C}_{i,j} & i \neq j \end{cases}. \quad (6)$$

In Equation (6), $\mathbf{J}_e^A(\mathbf{p}_k)$ and \mathbf{C}_{kj} represent the RI of agent k , which is observed from all the anchors and the agent j separately. They can be expressed by the following:

$$\mathbf{J}_e^A(\mathbf{p}_k) = \sum_{j \in \mathcal{A}_s} \lambda_{kj} \mathbf{q}_{kj} \mathbf{q}_{kj}^T, \quad (7)$$

$$\mathbf{C}_{kj} = \mathbf{C}_{jk} = (\lambda_{kj} + \lambda_{jk}) \mathbf{q}_{kj} \mathbf{q}_{kj}^T, \quad (8)$$

where $\mathbf{q}_{kj} = [\cos(\phi_{kj}), \sin(\phi_{kj})]^T$ illustrates the angular information between anchor k and agent j . The fundamental limits of localization performance are determined by SPEB, and thus, it is utilized as the performance metric in our work.

3. Eavesdropping Strategies Based on the Proposed Scheduling Framework

In this part, we introduced the eavesdropper to the network. If the localization strategy is appropriately adopted, some specific nodes in the sensor network do not need to transmit

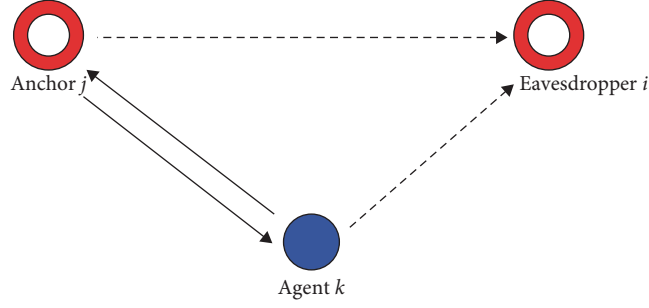


FIGURE 2: Network graph with dedicated eavesdropper.

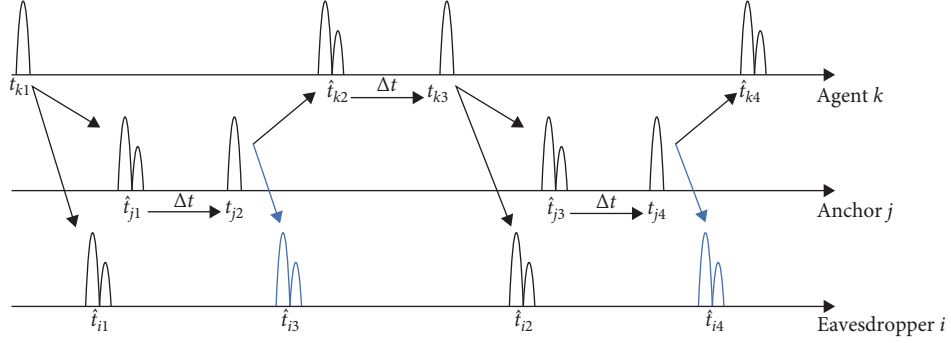


FIGURE 3: The flow chart of time about dedicated eavesdropper.

signals. Those eavesdroppers only need to “listening” the interaction of other nodes, and the system performance can be optimized, which is called eavesdropping. Thus, we build the scheduling policy for two scenarios as follows.

We proposed two eavesdropping strategies for wireless cooperative localization networks. The first strategy involves the use of a dedicated eavesdropper, as shown in Figure 2, which is a node with a known position that does not transmit signals but instead listens to the interaction of other nodes. The second strategy involves the use of eavesdropping anchors, where some or all anchors are equipped with listening capabilities and can overhear the information exchange between other nodes, as shown in Figure 3. Both strategies aim to improve system performance by optimizing resource allocation and scheduling.

3.1. Scheduling with the Dedicated Eavesdropper. As shown in Figure 2, a sensor network with *three* nodes is presented, where node *k* is the agent, *j* is the anchor, and *i* represents the *dedicated* eavesdropper. Figure 4 illustrates a conventional scheduling strategy. According to Equation (2), three RTMs of TOA are performed by the anchor and agent to estimate the distance d_{kj} . Meanwhile, the eavesdropper *i* does not send any signals during the RTMs processing, but it can receive the signals from other nodes. With the scheduling strategy illustrated in Figure 5, the signals can be collected to node *i*. Thus, the time difference is as follows:

$$\hat{t}_{i2} - \hat{t}_{i1} = 2 \cdot \Delta t + 2 \cdot \frac{\hat{d}_{kj}}{c}, \quad (9)$$

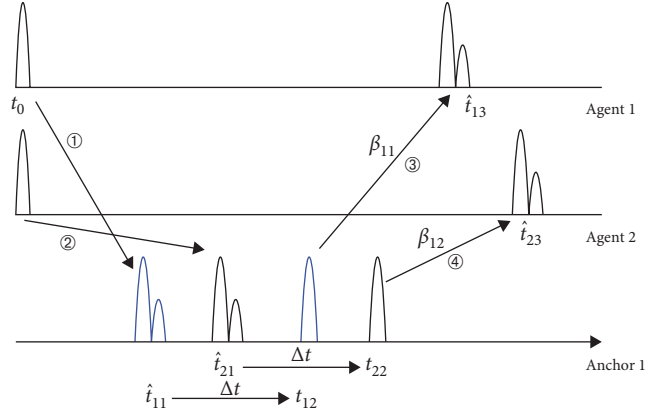


FIGURE 4: Round trip measurements of point to point transmission.

and the estimation of d_{kj} could be derived by the following:

$$\hat{d}_{kj} = c \cdot \frac{(\hat{t}_{i2} - \hat{t}_{i1}) - 2\Delta t}{2}. \quad (10)$$

For the observed RI at the eavesdropper, there exist cumulative errors, as shown in Figure 4. The error for \hat{t}_{i2} obtained at the eavesdropper can be affected by the transmitted signal from agent *k* at different times, like t_{k3} , \hat{t}_{k2} , and \hat{t}_{j1} . Therefore, the estimate at time t_{i2} is as follows:

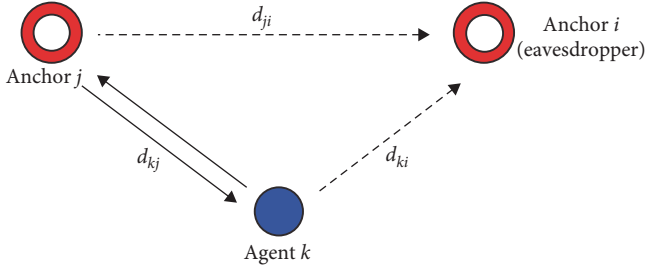


FIGURE 5: Network graph with eavesdropping anchors.

$$\begin{aligned}
 \widehat{t}_{i2} &= t_{i2} + e_{i2} \\
 &= t_{k3} + \frac{d_{ki}}{c} + e_{i2} \\
 &= t_{k2} + e_{k2} + \Delta t + \frac{d_{ki}}{c} + e_{i2} \\
 &= t_{j1} + e_{j1} + \Delta t + \frac{d_{kj}}{c} + e_{k2} + \Delta t + \frac{d_{ki}}{c} + e_{i2}
 \end{aligned} \quad (11)$$

where e_{j1} , e_{k2} , and e_{i2} are used to indicate the measurement errors. The variance for \widehat{d}_{kj} at eavesdropper is as follows:

$$\sigma_{e\text{-agent}}^2 = \frac{1}{4} [\sigma_{i1\text{-total}}^2 + \sigma_{i2\text{-total}}^2], \quad (12)$$

where

$$\sigma_{i1\text{-total}}^2 = \sigma_{i1}^2, \quad (13)$$

$$\sigma_{i2\text{-total}}^2 = \sigma_{j1}^2 + \sigma_{k2}^2 + \sigma_{i2}^2. \quad (14)$$

Meanwhile, the signals from anchors can be heard by eavesdroppers as well, i.e.,

$$\widehat{d}_{kj} = c \cdot \frac{(\widehat{t}_{i4} - \widehat{t}_{i3}) - 2\Delta t}{2}. \quad (15)$$

The corresponding variance is as follows:

$$\sigma_{e\text{-anchor}}^2 = \frac{1}{4} [\sigma_{i3\text{-total}}^2 + \sigma_{i4\text{-total}}^2], \quad (16)$$

where

$$\sigma_{i3\text{-total}}^2 = \sigma_{i3}^2 + \sigma_{j1}^2, \quad (17)$$

$$\sigma_{i4\text{-total}}^2 = \sigma_{i4}^2 + \sigma_{j3}^2 + \sigma_{k2}^2 + \sigma_{j1}^2, \quad (18)$$

$$\lambda_{e\text{-agent}} = \frac{1}{\sigma_{e\text{-agent}}^2} = \frac{4\xi_{ki}\xi_{kj}P_{k3}\beta_{k3}^2P_{j2}\beta_{j2}^2P_{k1}\beta_{k1}^2}{\xi_{ki}d_{kj}^q(P_{k1}\beta_{k1}^2 + P_{j2}\beta_{j2}^2)P_{k3}\beta_{k3}^2 + \xi_{kj}d_{ki}^q(P_{k1}\beta_{k1}^2 + P_{k3}\beta_{k3}^2)P_{j2}\beta_{j2}^2}, \quad (19)$$

$$\begin{aligned}
 \lambda_{e\text{-anchor}} &= \frac{1}{\sigma_{e\text{-anchor}}^2} = \frac{4\xi_{ji}\xi_{kj}(P_{k1}\beta_{k1}^2P_{k3}\beta_{k3}^2P_{j2}\beta_{j2}^2P_{j4}\beta_{j4}^2)}{\xi_{kj}d_{ji}^q(P_{j2}\beta_{j2}^2 + P_{j4}\beta_{j4}^2)P_{k1}\beta_{k1}^2P_{k3}\beta_{k3}^2} \\
 &\quad + \xi_{ji}d_{kj}^q(P_{k1}\beta_{k1}^2P_{k3}\beta_{k3}^2 + P_{j2}\beta_{j2}^2P_{k1}\beta_{k1}^2 + 2P_{k3}\beta_{k3}^2P_{j2}\beta_{j2}^2)P_{j4}\beta_{j4}^2
 \end{aligned} \quad (20)$$

It is noticeable that the network is assumed to be processed in a centralized manner. Observed range estimation needs to be transmitted to the center processor and then improve the network performance. Based on the definition, the RII of all estimations are able to be acquired in Equations (19) and (20).

Remark 1. Although the eavesdropper can realize distance estimation with no need for transmit power, it still needs twice estimates as much as RTMs (four versus two). Therefore, it can be deduced that the result of eavesdropping is less “reliable” than RTM, and the ranging accuracy is still mainly determined by RTMs. But on the other hand, for scenes with constrained energy and resources, eavesdroppers could be valuable.

The scene in Figure 4 is extended to a multinode scene here. One significant challenge here is that, because of the existence of multiple anchors and agents, the eavesdropper can hardly pair the received signal correctly. According to Song et al. [36], a frequency division multiplexing (FDM) method is applied in this scene, as shown in Figure 5, and thus the received signals can be recognized with their frequency bands. The strategy can be concluded as follows:

- (i) Initialization: With a *point-to-point* manner, RTMs are initialized at all the nodes, while the frequency bands are preallocated [35]. The procedure is happened in the first time slot.

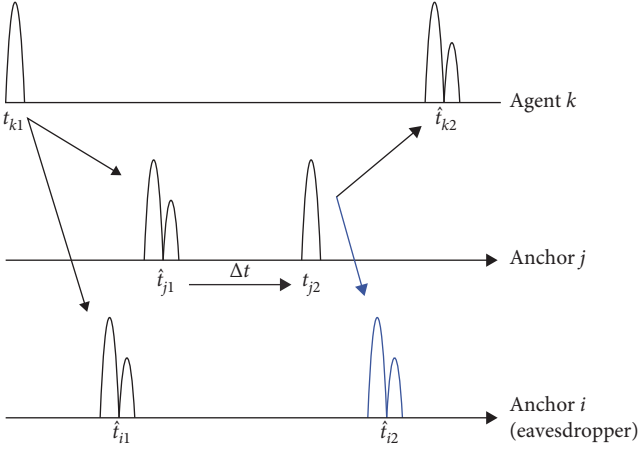


FIGURE 6: The flowchart of time about anchor eavesdropping.

- (ii) Replication: In the second time slot, the signals are replied from the anchors with FDM method to realize TOA-based RTM.
- (iii) Eavesdropping: In the third and fourth time slot, the signals transmitted from other nodes are overheard by the eavesdropper, and one measurement consists of four time slots. This measurement will not stop until the system is turned off.

3.2. Scheduling Strategy with Eavesdropping Anchors. In this part, we present another eavesdropping method according to the allocation framework in Figure 5. As shown in Figure 3, there is a simple distribution of nodes in a location network, where d_{kj} represents the range difference from agent k to anchor j , which can be gotten from an RTM. d_{ji} represents the distance between anchor j and eavesdropper i . Here, we assume that the eavesdropper is an anchor whose location is known. Therefore, we can derive d_{ji} .

Based on the scheduling strategy with eavesdropping anchors in Figure 6, node i can receive all the RI from agent k and anchor j . So we can see that,

$$\begin{aligned} \hat{t}_{i2} - \hat{t}_{i1} &= \frac{d_{kj}}{c} + \Delta t + \frac{d_{ji} - \hat{d}_{ki}}{c} \\ &= \frac{1}{2} [(\hat{t}_{k2} - t_{k1}) - (t_{j2} - \hat{t}_{j1})] + \Delta t + \frac{d_{ji} - \hat{d}_{ki}}{c}, \end{aligned} \quad (21)$$

by which an estimate of d_{ki} can be obtained by the following:

$$\begin{aligned} \hat{d}_{ki} &= \frac{c}{2} [(\hat{t}_{k2} - t_{k1}) - (t_{j2} - \hat{t}_{j1})] + c \cdot \Delta t \\ &\quad + d_{ji} + c \cdot (\hat{t}_{i2} - \hat{t}_{i1}) \end{aligned}, \quad (22)$$

where

$$\hat{t}_{k2} = t_{k2} + e_{k2}, \quad (23)$$

$$\hat{t}_{j1} = t_{j1} + e_{j1}, \quad (24)$$

$$\hat{t}_{i1} = t_{i1} + e_{i1}, \quad (25)$$

$$\hat{t}_{i2} = t_{i2} + e_{i2}. \quad (26)$$

According to Section 3.1, we can calculate the variance as follows:

$$\sigma_e^2 = \frac{1}{4} [\sigma_{k2}^2 + \sigma_{j1}^2] + (\sigma_{i2}^2 + \sigma_{j1}^2) + \sigma_{i1}^2, \quad (27)$$

$$\lambda_e = \frac{1}{\sigma_e^2}$$

$$= \frac{4\xi_{ki}\xi_{kj}\xi_{ji}P_{k1}\beta_{k1}^2P_{j2}\beta_{j2}^2}{\xi_{ki}(\xi_{ji}d_{kj}^0 + 4\xi_{kj}d_{ji}^0)P_{k1}\beta_{k1}^2 + \xi_{ji}(5\xi_{ki}d_{kj}^0 + 4\xi_{kj}d_{ki}^0)P_{j2}\beta_{j2}^2}. \quad (28)$$

It is noticeable that for all the eavesdroppers, there exists cumulative error from localization signals, and the variance of \hat{t}_{i2} can be calculated similarly to Equation (11). According to the formula, we can see that the eavesdropper i could obtain the RI between agent k and itself by eavesdropping the RTM signals of agent k and anchor j . If some anchors turn to eavesdroppers, the ranging performance of the whole system will be optimized. Based on the definition, Equation (28) can derive the RII for all the estimations.

4. Resource Allocation and Optimization Algorithms

Our work mainly includes two aspects. In the first step, we present a new network scheduling strategy, i.e., we build a rule about how the whole network works. Based on the presented strategy, the value of an eavesdropper is more like a dedicated "listener" or specific anchor. Then, in the second step, when the resources, including power and bandwidth, are subject to constraints, we perform resource optimization using a Taylor expansion-based high-accuracy approximate algorithm. With relatively few times of iteration, the non-convex question can be approximated to a linear problem.

4.1. Dedicated Eavesdropper Cases. A dedicated eavesdropper is a node that has a known position but can not send signals, i.e., it does not occupy system resources. Since the RII is determined by the transmitted energy and frequency bandwidth, we set the objective function based on the global SPEB. By optimizing the joint power and bandwidth allocation of all the nodes, the objective function could be minimized. The total power limit of agents and anchors is limited, while the individual power limit is also given. The optimization problems can be presented as follows:

$$\mathcal{P}_1: \min. \sum_{k \in \mathcal{N}_a} \mathcal{P}(\mathbf{p}_k), \quad (29)$$

$$\text{s.t. } 0 \leq P_{k,j}^{(2t-1)} + P_{k,l}^{(2t-1)}, P_{j,k}^{(2t)}, P_{l,k}^{(2t)} \leq P_0, \quad (30)$$

$$\sum_{t=1}^{N_t} \left(\sum_{k=1}^{N_a} \sum_{j=1}^{N_b} P_{k,j}^{(2t-1)} + \sum_{k,l=1}^{N_a} P_{k,l}^{(2t-1)} + \sum_{k,l=1}^{N_a} P_{l,k}^{(2t)} \right) \leq P_{\text{agent}}, \quad (31)$$

$$\sum_{t=1}^{N_t} \left(\sum_{j=1}^{N_b} \sum_{k=1}^{N_a} P_{j,k}^{(2t)} \right) \leq P_{\text{anchor}}, \quad (32)$$

$$\sum_{k=1}^{N_a} \sum_{l=1}^{N_a} \beta_{l,k}^{(2t-1)} + \sum_{j=1}^{N_b} \sum_{k=1}^{N_a} \beta_{j,k-\text{RTM}}^{(2t-1)} \leq B_0, \quad (33)$$

$$\sum_{k=1}^{N_a} \sum_{l=1}^{N_a} \beta_{l,k}^{(2t)} + \sum_{j=1}^{N_b} \sum_{k=1}^{N_a} \beta_{j,k-\text{RTM}}^{(2t)} \leq B_0, \quad (34)$$

where \mathcal{N}_a is the number of agents and \mathcal{N}_b is the number of anchors, $k, l \in \mathcal{N}_a$, $j \in \mathcal{N}_b$, $t \in \{1, 2, \dots, N_t\}$. $P_{k,j}^{(2t-1)}$ and $\beta_{k,j}^{(2t-1)}$ are the transmit power and bandwidth from agent k to anchor j at the odd time slots, $P_{k,l}^{(2t-1)}$ and $\beta_{k,l}^{(2t-1)}$ are the transmit power and bandwidth from agent k to cooperative agent l at the odd time slots. Similarly, $P_{j,k}^{(2t)}$ and $\beta_{j,k}^{(2t)}$ are the transmit power and bandwidth from anchor j to agent k at even time slots, $P_{l,k}^{(2t)}$ and $\beta_{l,k}^{(2t)}$ are the transmit power and bandwidth from cooperative agent l to agent k at even time slots, respectively. P_0 and B_0 are the power and bandwidth limits for each node, while P_{agent} and P_{anchor} are the whole power bound for all the agents and anchors, respectively. $\mathcal{P}(\mathbf{p}_k)$ in Equation (29) is obtained from both RTMs and eavesdropping, i.e.,

$$\begin{aligned} \mathcal{P}(\mathbf{p}_k) &= \text{tr}\{\mathbf{J}_{\text{RTM}}(\mathbf{p}_k) + \mathbf{J}_e(\mathbf{p}_k)\}^{-1} \\ &= \text{tr}\left\{ \mathbf{J}_{\text{RTM}}(\mathbf{p}_k) + \sum_{j \in \mathcal{N}_b} \lambda_{kj}^{\text{e-agent}} \mathbf{q}_{kj} \mathbf{q}_{kj}^T \right. \\ &\quad \left. + \sum_{j \in \mathcal{N}_b} \lambda_{kj}^{\text{e-anchor}} \mathbf{q}_{kj} \mathbf{q}_{kj}^T - \mathbf{I} \right\}^{-1}. \end{aligned} \quad (35)$$

We can see from Equation (35) that the RI can be obtained from two aspects. We could obtain it according to perform RTMs with anchors, i.e., $\mathbf{J}_{\text{RTM}}(\mathbf{p}_k)$. At the same time, the eavesdropper can also obtain the location information, i.e., $\mathbf{J}_e(\mathbf{p}_k)$, which include the information “listening” from anchor and agent. Note that when there is no eavesdropper, $\mathbf{J}_e(\mathbf{p}_k)$ will become zero, and the location system will transfer to the conventional RTMs.

In Equation (29) of \mathcal{P}_1 , the aim is to minimize the SPEB of all nodes by adopting proper allocation methods. The constraints in Equation (31) limit the maximum power given to each node, while Equations (31) and (32) present the power limits for the whole network respectively for a N_t time measurement. Besides, the bandwidth limitation is given in Equations (33) and (34) to avoid interference in even and odd time slots separately.

4.2. Eavesdropping Anchors. Consider another strategy of eavesdropping in the scheduling framework based on Figure 6. i.e., dedicated eavesdroppers are no longer added to the wireless positioning network, but some or all anchors are provided with “listening” function. While the “anchor” joins in RTM, it can also listen to the information exchange between other nodes. Based on the eavesdropping scheduling policy of the anchor with the eavesdropping ability, the optimization problem in \mathcal{P}_1 could be rewritten as \mathcal{P}_2 .

$$\mathcal{P}_2 : \min. \sum_{k \in \mathcal{N}_a} \mathcal{P}(\mathbf{p}_k), \quad (36)$$

$$\text{s.t. } (30) - (34), \quad (37)$$

$$\beta_{j,k-\text{RTM}} + \beta_{j,k-e} \leq \beta_{j,k}, \quad (38)$$

where $\beta_{j,k-e}$ and $\beta_{j,k-\text{RTM}}$ are the bandwidth from agent k to anchor j for RTM and eavesdropping, respectively, and $\beta_{j,k}$ is the bandwidth of corresponding agent–anchor pair. It is noticeable that, because of the use of half-duplex transceivers in practical cases, only different band signals can be received at the eavesdroppers. Thus, Equation (38) is presented here. Obviously, if anchors do not have the ability to eavesdrop, $\beta_{j,k-e}$ will be zero. $\mathcal{P}(\mathbf{p}_k)$ in Equation (36) can be acquired from both RTMs and eavesdropping, i.e.,

$$\begin{aligned} \mathcal{P}(\mathbf{p}_k) &= \text{tr}\{\mathbf{J}_{\text{RTM}}(\mathbf{p}_k) + \mathbf{J}_e(\mathbf{p}_k)\}^{-1} \\ &= \text{tr}\left\{ \mathbf{J}_{\text{RTM}}(\mathbf{p}_k) + \sum_{j \in \mathcal{N}_b, j \neq i} \lambda_{kj}^e \mathbf{q}_{kj} \mathbf{q}_{kj}^T \right\}^{-1}. \end{aligned} \quad (39)$$

4.3. Anchor Eavesdropping with Power Consuming. The anchor with the eavesdropping function mentioned above does not generate power consumption while “listening,” but in the actual situation, once the node is in the open mode, it generates power consumption; that is, the anchor has the following three modes, including sleep, eavesdropping, and distance measurement. In sleep mode, no power consumption is generated, while under the function of eavesdropping, the node wakes up and thus has a fixed power consumption. By considering the above conditions, limiting the sum of total power, the \mathcal{P}_2 can be modified as follows:

$$\mathcal{P}_3 : \min \sum_{k \in \mathcal{N}_a} \mathcal{P}(\mathbf{p}_k), \quad (40)$$

$$\text{s.t. } (37) - (38), \quad (41)$$

$$\sum_{k=1}^{N_a} \sum_{j=1}^{N_b} P_{k,j-\text{RTM}} + \sum_{k=1}^{N_a} \sum_{j=1}^{N_b} P_{k,j-e} \leq P_{\text{anchor}}, \quad (42)$$

where $P_{k,j-\text{RTM}}$ and $P_{k,j-e}$ are the power for agent k to anchor j , for RTM and eavesdropping respectively, while P_{agent} is the power of corresponding agent. $\mathcal{P}(\mathbf{p}_k)$ in Equation (40) is as follows:

$$\mathcal{P}(\mathbf{p}_k) = \text{tr}\{\mathbf{J}_{\text{RTM}}(\mathbf{p}_k) + \gamma \cdot \mathbf{J}_e(\mathbf{p}_k)\}^{-1}, \quad (43)$$

where parameter γ indicates whether to enable the anchor node. Since we consider the power consumption of eavesdroppers, constraint Equation (42) is added to limit the peak transmit power.

Note that \mathcal{P}_1 , \mathcal{P}_2 , and \mathcal{P}_3 are non-convex due to the form of RII. Thus, we need to introduce an approximate method to solve this problem. First-order Taylor expansion can be adopted to a certain point of λ_{kj} . According to Zhang et al. [41], the RII can be derived as follows:

$$\begin{aligned} \lambda_{kj}(x, \theta) &\approx \lambda_{kj}^{TL}(x, \theta) \\ &= \lambda_{kj}(x^{(m-1)}, \theta^{(m-1)}) + \nabla_x \lambda_{kj}(x^{(m-1)}) \Delta x, \\ &\quad + \nabla_\theta \lambda_{kj}(\theta^{(m-1)}) \Delta \theta \end{aligned} \quad (44)$$

combined with the trust region constraint

$$[\theta - \theta^{(m-1)}] = \|\Delta \theta\| \leq R_\theta^{(m)}, \quad (45)$$

where θ represents all parameters to be optimized. m is the index of iteration. $R_\theta^{(m)}$ is radius of the trust regions at m th iteration.

5. Numerical Results

In this section, we discuss the simulated results of the scheduling problems based on the former methods. It is assumed that all nodes power are normalized, which means $P_{\text{anchor-RTM}} = P_{\text{agent-RTM}} = 1$, while the bandwidth limit of one individual time slot is also $B_0 = 1$. A 10×10 square area U is covered by the wireless localization network, which contains N_a agents and N_b anchors. The IEEE 802.15.4a CM1 channel model is adopted here to derive the channel coefficient. The probability of shadowing between two nodes is set to 0.5. All scheduling problems are solved by the standard solver package CVX [42].

5.1. Multislot Scheduling. In order to eavesdrop more information, the RTM can be extended in multislot. In the case of two complete RTMs, two, three, and four time slots are simulated separately. We enable the three anchors to overhear signals. In order to verify the generality of the experimental conclusions, a single agent is randomly generated multiple times in a square region, wherein the positioning network accuracy varies with the number of time slots, as shown in Table 1. N_t indicates the number of time slots.

Table 1 leads us to the conclusion that (i) as the number of time slots increases, the system-squared positioning error bound tends to decrease. Since the bandwidth resources are reallocated every time slot, the accuracy of the positioning network increases as the number of time slots increases. (ii) Also, it can be seen that, with the increasing of the number of time slots, the improving trend of the positioning accuracy of the position system is not obvious, since the system error

TABLE 1: Positioning accuracy in multislot eavesdropping.

N_t	2	3	4
SPEB (m ²)	0.072	0.0490	0.0425

TABLE 2: Power allocation of each time slot in four-slot listening.

S_t	1st	2nd	3rd	4th
Allocated power	0.8	0.095	0.055	0.05

reduction is only about 0.02 m². When the number of positioning slots increases to 3, the system positioning error is reduced by 31.94%, and when the number of positioning slots increases to 4, the system positioning error is only reduced by 13.27%; the reduction ratio shows a significant downward trend.

In order to explain this phenomenon, the number of system positioning time slots is set to 4, and multiple experimental data are counted. The average power distribution of each time slot is shown in Table 2, where S_t indicates the serial number of time slot. The following conclusions can be drawn as follows:

- (i) It can be seen that the power is mainly divided into the first time slot, and the power allocated by the remaining three time slots is less than 0.1, i.e., the power allocation has obvious sparsity.
- (ii) As the time slot increases, the positioning error is also cumulative, so the power distribution does not appear in a uniformly distributed form.
- (iii) Since the accuracy of the positioning network, with the increase of the number of positioning slots, does not greatly improve, the detection based on three time slots or more is of little significance.

5.2. Performance Analysis of Introducing Dedicated Eavesdroppers.

In order to analyze the impact of the introduction of dedicated eavesdroppers on the performance of the wireless positioning network, the distribution of nodes in the positioning network is shown in Figure 7, and the distribution of the anchors is approximated by a straight line. Based on the dual-slot scheduling strategy, the simulation result is given (as shown in Figure 8), the abscissa is used to measure the network positioning accuracy, and the ordinate is the cumulative probability distribution. Figure 8 illustrates the following:

- (i) The introduction of the dedicated eavesdropper can ensure that the 95% probability system positioning error is lower than 0.11 m², and the pure RTM can only ensure that the system positioning error is lower than 0.52 m².
- (ii) When the system resources are the same, the positioning accuracy of a wireless positioning network with a dedicated eavesdropper is significantly better than that of the pure RTM.

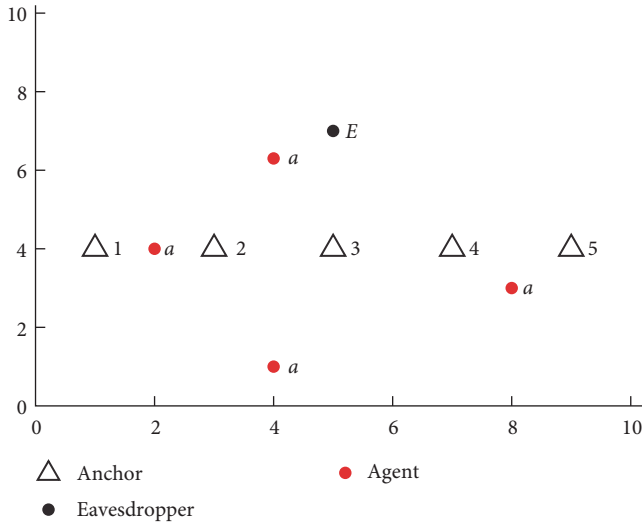


FIGURE 7: Scene with poor anchor node distribution.

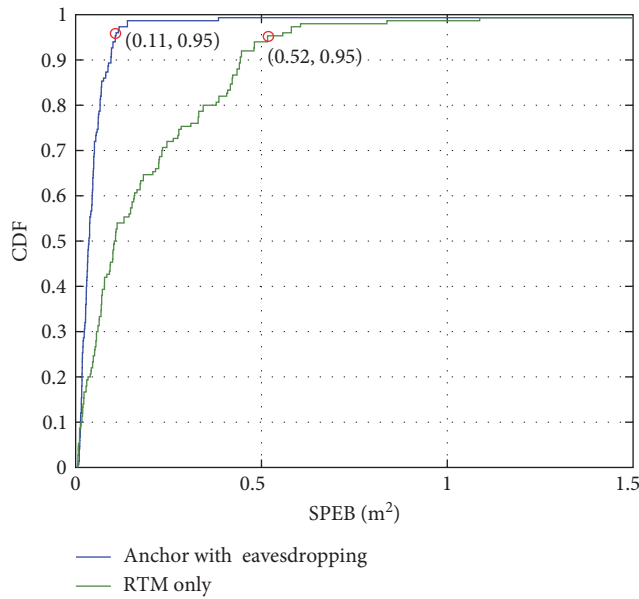


FIGURE 8: Localization accuracy with dedicated eavesdropper.

- (iii) When the distribution of anchors in the network is unreasonable, and the agent is difficult to locate, the dedicated eavesdropper can be broadcasted to assist the ranging. Because it consumes less power and can provide a better measurement angle to assist distance measurement.

Furthermore, a special case is presented here. As shown in Figure 9, there are three anchors, one agent, and one eavesdropper posed inside the area. The shadowing effects between anchors and agents are presented. To simplify, the shadowing probability is 0.5, while the power attenuation varies from 0–20 dB. The SIMULATED results are shown in Figure 10. We can see the following:

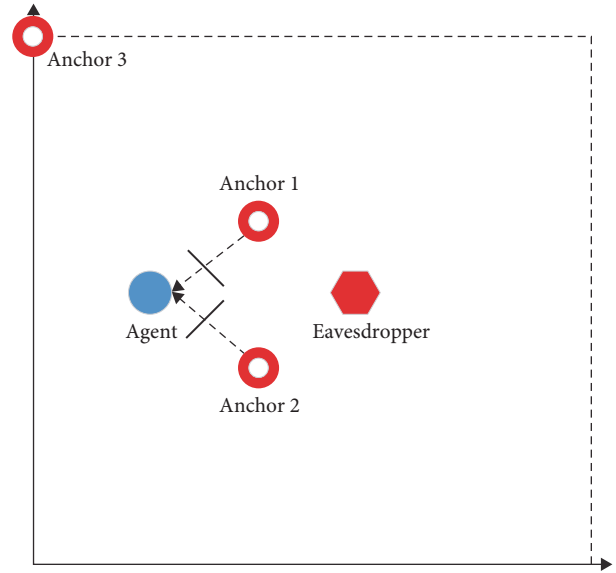


FIGURE 9: A special network deployment.

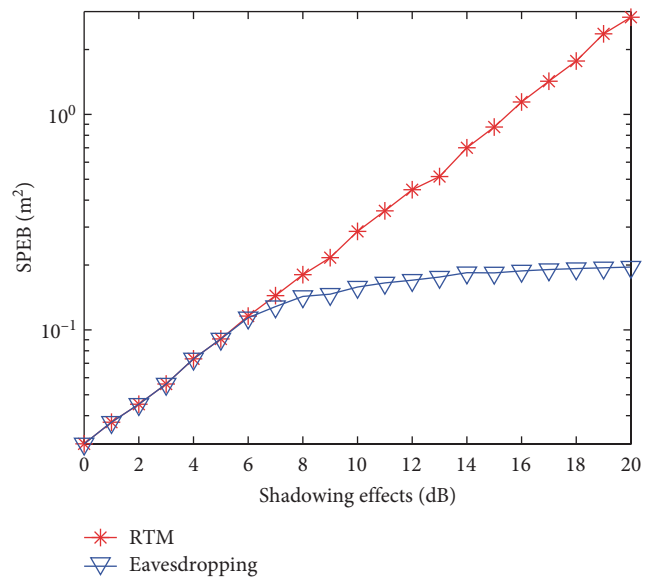


FIGURE 10: Accuracy results in a special situation.

- (i) With a low-shadowing effect, the position of the agent is primarily determined by the distance estimation of the two nearby anchors. Eavesdroppers have a relatively lower influence.
- (ii) With the attenuation of signal attenuation increasing (larger than 15 dB in the investigated cases), the results of eavesdroppers tend to be valuable.
- (iii) Similar to Remark 1, the localization performance is mainly determined by RTM results. However, if the DP signal cannot be received, eavesdroppers are helpful to increase ranging accuracy.

5.3. Performance Analysis of Eavesdropping Anchors. This section mainly considers the scene where the anchor has the

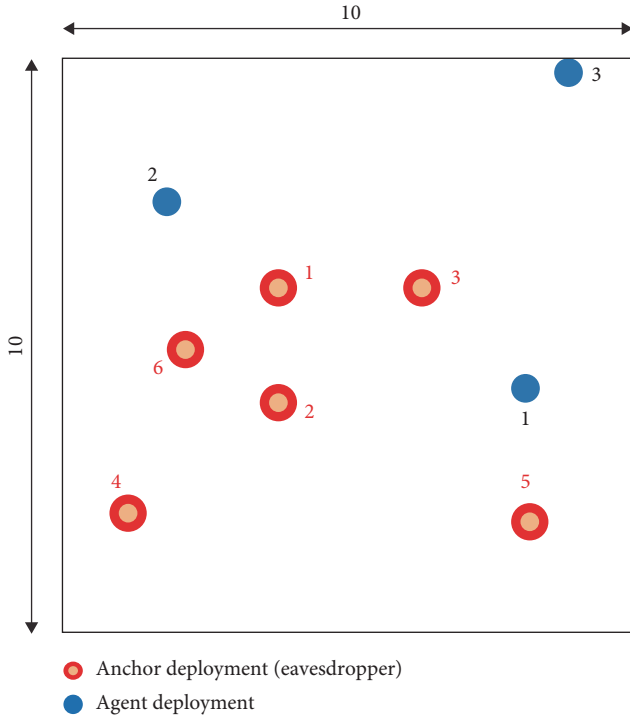


FIGURE 11: Anchor distribution map with eavesdropping function.

eavesdropping function. It should be noted that since the half-duplex signal transmission method is usually adopted in practice, the anchor equipped with an eavesdropping function must use different frequency bands to transmit or receive signals at the same time. The distribution of network nodes is shown in Figure 11, that is, six fixed position anchors and three random agents. All simulations performed two complete RTMs, and the total power and bandwidth resources in the wireless positioning network are the same. Figure 12 shows a comparison between the positioning accuracy of the anchor with the eavesdropping function and the positioning accuracy of pure RTM.

As is demonstrated in Figure 12, the network localization accuracy achieved by the eavesdropping anchors is generally better than the traditional RTM-based system. It can be seen that when the anchor has eavesdropping function, the square error of the positioning network is 95% $< 7.6 \text{ m}^2$, and RTM can only guarantee that 95% probability square error is $< 20 \text{ m}^2$.

According to Equations (34) and (38), the total bandwidth available is fixed. So, it will be a tradeoff whether the anchors perform eavesdropping or not. Under the defined wireless position network, a bandwidth indicator for eavesdropping (η) is defined as follows:

$$\eta = \frac{\beta_{\text{eavesdropping}}}{\beta_{\text{RTM}} + \beta_{\text{eavesdropping}}} \quad (46)$$

which indicates the ratio of bandwidth that the anchor allocates for eavesdropping.

As shown in Figure 13, the conclusions can be drawn as follows:

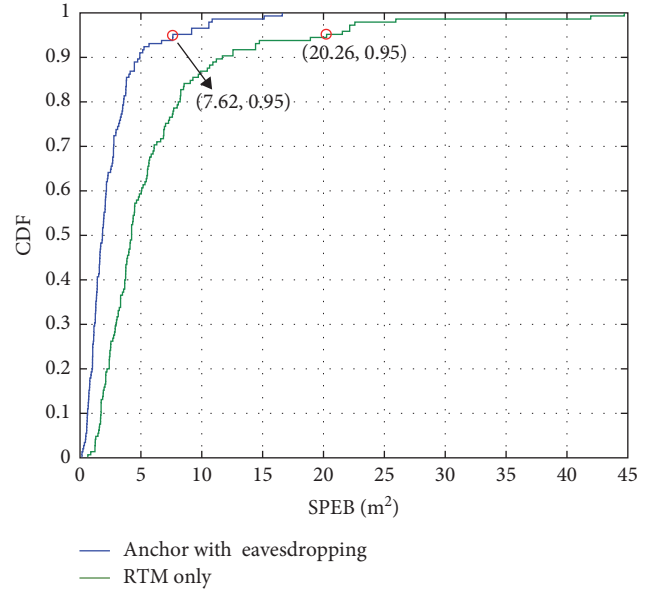


FIGURE 12: Positioning system's accuracy with eavesdropping anchor.

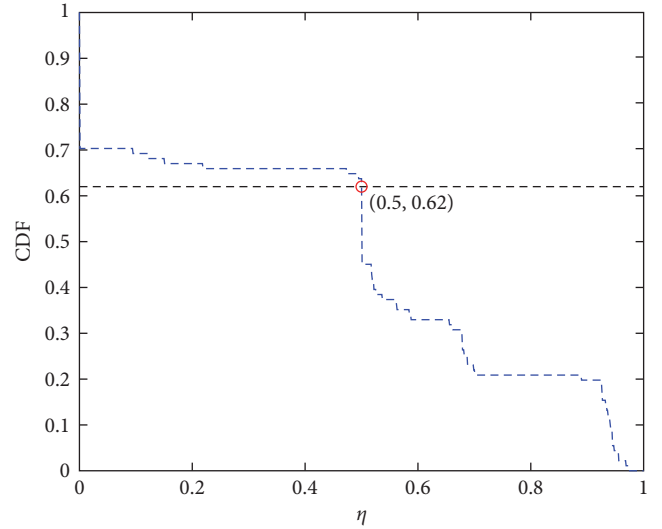


FIGURE 13: CDF with respect to bandwidth allocation parameters.

- (i) Observing the intersection of the image and the vertical axis, it can be seen that the positioning network will enable the eavesdropping function with the probability exceeding 70%.
- (ii) Then, by making an auxiliary line parallel to the horizontal axis, it can be seen that the anchor has a probability of 62% that it will use 50% of the total system bandwidth for eavesdropping.
- (iii) When the anchor is equipped with the eavesdropping function, the idle bandwidth can be used to listen to signals sent by surrounding nodes to obtain positioning information. Because the eavesdropping consumes less power and the eavesdropper does not send a signal to interfere the surroundings. The

result of the system optimization is that more than half of the bandwidth is allocated for eavesdropping in most cases. Thus, eavesdropping anchors can provide highly energy-efficient ranging results.

6. Conclusion

In this paper, based on the nondata-aided scheduling strategy, we show that eavesdropper is helpful in asynchronous localization networks. Firstly, we present an eavesdropping scheduling policy. Then, a resource optimization scheme based on the scheduling strategy is performed, and a high-accuracy algorithm is proposed to solve the resource allocation problem. According to the numerical results, we can see the following:

- (i) Eavesdropping could improve the system performance without extra transmitting signals, which is valuable in energy-constraint scenarios. For the scenario with block RTMs, the localization error with dedicated eavesdroppers is only 21% of the conventional networks. Besides, the system with eavesdropping anchors could improve the localization performance than 70%.
- (ii) Appropriate resource allocation is essential for the system's performance when the total resources are limited.
- (iii) The localization task is mainly based on the traditional RTMs. However, when the network is poorly deployed or the signals are severely attenuated, eavesdropping is a reliable substitute to increase ranging performance. These proposed strategies and numerical results may be helpful for practical LBS system design.

Although our strategies could improve the performance of wireless cooperative localization networks through the use of eavesdropping and resource optimization, there are still many avenues for future research in this area. For example, further investigation could be conducted to determine the impact of these approaches on dense networks operating under global resource limitations. Additionally, new algorithms and techniques could be developed to improve the efficiency and accuracy of eavesdropping and resource allocation or to address challenges such as severe obstacles blocking the anchors. By building on the current work and extending it in new and innovative ways, we can further improve their performance in real-world scenarios.

Data Availability

The data used to support the findings of this study are included within the article.

Conflicts of Interest

The authors declare that they have no conflicts of interest.

Acknowledgments

This paper was supported by the Natural Science Foundation of China (NSFC) under Grant Nos. 62171160, 91638204, and 61101124, the Natural Science Foundation of Shenzhen under Grant No. JCYJ20160531192013063, The Domestic Joint Postgraduate Training Project (LHPY-2021005), the Scientific Research Project in School-Level (SZIIT2019KJ026), the Fundamental Research Funds for the Central Universities under Grant No. HIT.OCEF.2022055, and the Shenzhen Science and Technology Program under Grant Nos. JCYJ20190806143212658 and ZDSYS20210623091808025, and also a major project of PCL.

References

- [1] X. Yu, T. Zhang, L. Song, and Q. Zhang, "Eavesdropping in wireless localization networks using round trip measurements," in *2016 IEEE 17th International Workshop on Signal Processing Advances in Wireless Communications (SPAWC)*, pp. 1–5, 2016.
- [2] W. You, F. Li, L. Liao, and M. Huang, "Data fusion of UWB and IMU based on unscented kalman filter for indoor localization of quadrotor UAV," *IEEE Access*, vol. 8, pp. 64971–64981, 2020.
- [3] C. E. O'Lone, H. S. Dhillon, and R. M. Buehrer, "A statistical characterization of localization performance in wireless networks," *IEEE Transactions on Wireless Communications*, vol. 17, no. 9, pp. 5841–5856, 2018.
- [4] Bo Gao, Mu Jia, Tingting Zhang, and Qinyu Zhang, "Reliable target positioning in complicated environments using multiple radar observations," in *2021 IEEE Global Communications Conference (GLOBECOM)*, pp. 1–6, 2021.
- [5] C. Laoudias, A. Moreira, S. Kim, S. Lee, L. Wirola, and C. Fischione, "A survey of enabling technologies for network localization, tracking, and navigation," *IEEE Communications Surveys & Tutorials*, vol. 20, no. 4, pp. 3607–3644, 2018.
- [6] X. Wang, M. Jia, X. Meng, and T. Zhang, "Multipath ghosts mitigation for radar-based positioning systems," in *2022 IEEE 96th Vehicular Technology Conference (VTC2022-Fall)*, pp. 1–6, 2022.
- [7] M. Jia, S. Li, J. le Kerneec, Y. Yang, F. Fioranelli, and O. Romain, "Human activity classification with radar signal processing and machine learning," in *2020 International Conference on UK-China Emerging Technologies (UCET)*, pp. 1–5, 2020.
- [8] J. Luo, Z. Zhang, C. Liu, and H. Luo, "Reliable and cooperative target tracking based on WSN and WiFi in indoor wireless networks," *IEEE Access*, vol. 6, pp. 24846–24855, 2018.
- [9] R. Mendrzik and G. Bauch, "Position-constrained stochastic inference for cooperative indoor localization," *IEEE Transactions on Signal and Information Processing over Networks*, vol. 5, no. 3, pp. 454–468, 2019.
- [10] Y.-Y. Li, G.-Q. Qi, and A.-D. Sheng, "Performance metric on the best achievable accuracy for hybrid TOA/AOA target localization," *IEEE Communications Letters*, vol. 22, no. 7, pp. 1474–1477, 2018.
- [11] K. Lam, C. Cheung, and W. Lee, "Rssi-based lora localization systems for large-scale indoor and outdoor environments," *IEEE Transactions on Vehicular Technology*, vol. 68, no. 12, pp. 11778–11791, 2019.
- [12] G. Wang, N. Ansari, and Y. Li, "A fractional programming method for target localization in asynchronous networks," *IEEE Access*, vol. 6, pp. 56727–56736, 2018.

- [13] A. Makki, A. Siddig, M. Saad, J. R. Cavallaro, and C. J. Bleakley, "Indoor localization using 802.11 time differences of arrival," *IEEE Transactions on Instrumentation and Measurement*, vol. 65, no. 3, pp. 614–623, 2016.
- [14] S. Bottigliero, D. Milanese, M. Saccani, and R. Maggiora, "A low-cost indoor real-time locating system based on TDOA estimation of UWB pulse sequences," *IEEE Transactions on Instrumentation and Measurement*, vol. 70, pp. 1–11, 2021.
- [15] F. Liu, T. Zhang, and P. Cao, "Asynchronous integration of communication and localization systems using ir-uwb signals," in *MILCOM 2021–2021 IEEE Military Communications Conference (MILCOM)*, pp. 521–527, 2021.
- [16] L. Barbieri, M. Brambilla, A. Trabattoni, S. Mervic, and M. Nicoli, "UWB localization in a smart factory: augmentation methods and experimental assessment," *IEEE Transactions on Instrumentation and Measurement*, vol. 70, pp. 1–18, 2021.
- [17] J. Zhu, S. Li, and J. Song, "Continuous human activity recognition with distributed radar sensor networks and CNN–RNN architectures," *IEEE Transactions on Geoscience and Remote Sensing*, vol. 60, pp. 1–12, 2022.
- [18] P. Mayer, M. Magno, and L. Benini, "Self-sustaining ultra-wideband positioning system for event-driven indoor localization," *IEEE Internet of Things Journal*, p. 1, 2023.
- [19] W. Dai, Y. Shen, and M. Z. Win, "Distributed power allocation for cooperative wireless network localization," *IEEE Journal on Selected Areas in Communications*, vol. 33, no. 1, pp. 28–40, 2015.
- [20] C. Yang, F. Liu, and T. Zhan, "Mse based resource optimization in wireless localization networks," in *2021 IEEE 93rd Vehicular Technology Conference (VTC2021-Spring)*, pp. 1–6, 2021.
- [21] Z. Liu, B. Liu, and C. W. Chen, "Joint power-rate-slot resource allocation in energy harvesting-powered wireless body area networks," *IEEE Transactions on Vehicular Technology*, vol. 67, no. 12, pp. 12152–12164, 2018.
- [22] J. Chen, W. Dai, Y. Shen, V. K. N. Lau, and M. Z. Win, "Resource management games for distributed network localization," *IEEE Journal on Selected Areas in Communications*, vol. 35, no. 2, pp. 317–329, 2017.
- [23] A. D. Sezer and S. Gezici, "Power control games between anchor and jammer nodes in wireless localization networks," *IEEE Transactions on Signal and Information Processing over Networks*, vol. 4, no. 3, pp. 564–575, 2018.
- [24] M. Ke, G. Zhao, S. Tian, C. Wang, and Y. Liu, "Optimal power allocation for anchor nodes in jammed wireless localization systems," *IEEE Wireless Communications Letters*, vol. 8, no. 4, pp. 1150–1153, 2019.
- [25] M. Jia, J. Yang, and T. Zhang, "Power allocation in infrastructure limited integration sensing and localization wireless networks," in *2022 IEEE 96th Vehicular Technology Conference (VTC2022-Fall)*, pp. 1–5, 2022.
- [26] T. Zhang, A. F. Molisch, Y. Shen, Q. Zhang, and M. Z. Win, "Joint power and bandwidth allocation in cooperative wireless localization networks," in *2014 IEEE International Conference on Communications (ICC)*, pp. 2611–2616, 2014.
- [27] T. Zhang, C. Qin, A. F. Molisch, and Q. Zhang, "Joint allocation of spectral and power resources for non-cooperative wireless localization networks," *IEEE Transactions on Communications*, vol. 64, no. 9, pp. 3733–3745, 2016.
- [28] J. Yang, T. Zhang, X. Wu, T. Liang, and Q. Zhang, "Efficient scheduling in space–air–ground-integrated localization networks," *IEEE Internet of Things Journal*, vol. 9, no. 18, pp. 17689–17704, 2022.
- [29] A. Liu, L. Lian, V. Lau, G. Liu, and M. Zhao, "Cloud-assisted cooperative localization for vehicle platoons: a turbo approach," *IEEE Transactions on Signal Processing*, vol. 68, pp. 605–620, 2020.
- [30] B. Peng, G. Seco-Granados, E. Steinmetz, M. Frohle, and H. Wymeersch, "Decentralized scheduling for cooperative localization with deep reinforcement learning," *IEEE Transactions on Vehicular Technology*, vol. 68, no. 5, pp. 4295–4305, 2019.
- [31] S. Salari, I. Kim, and F. Chan, "Distributed cooperative localization for mobile wireless sensor networks," *IEEE Wireless Communications Letters*, vol. 7, no. 1, pp. 18–21, 2018.
- [32] H. Wang, S. Tan, Y. Zhu, and M. Li, "Deterministic scheduling with optimization of average transmission delays in industrial wireless sensor networks," *IEEE Access*, vol. 8, pp. 18852–18862, 2020.
- [33] T. Wang, A. Conti, and M. Z. Win, "Network navigation with scheduling: distributed algorithms," *IEEE/ACM Transactions on Networking*, vol. 27, no. 4, pp. 1319–1329, 2019.
- [34] Q. Li, "Legitimate eavesdropping with wireless powered proactive full-duplex eavesdroppers," in *2021 IEEE Wireless Communications and Networking Conference (WCNC)*, pp. 1–6, 2021.
- [35] S. Dwivedi, A. De Angelis, and P. Handel, "Scheduled uwb pulse transmissions for cooperative localization," in *2012 IEEE International Conference on Ultra-Wideband*, pp. 6–10, 2012.
- [36] L. Song, T. Zhang, X. Yu, C. Qin, and Q. Zhang, "Scheduling in cooperative UWB localization networks using round trip measurements," *IEEE Communications Letters*, vol. 20, no. 7, pp. 1409–1412, 2016.
- [37] W. Dai, Y. Shen, and M. Z. Win, "Energy-efficient network navigation algorithms," *IEEE Journal on Selected Areas in Communications*, vol. 33, no. 7, pp. 1418–1430, 2015.
- [38] A. F. Molisch, K. Balakrishnan, D. Cassioli et al., "IEEE 802.15. 4a channel model-final report," *IEEE*, vol. 15, no. 4, pp. 1–41, 2004.
- [39] Y. Shen and M. Z. Win, "Fundamental limits of wideband localization—Part I: A general framework," *IEEE Transactions on Information Theory*, vol. 56, no. 10, pp. 4956–4980, 2010.
- [40] Y. Shen, H. Wymeersch, and M. Z. Win, "Fundamental limits of wideband localization Part II: Cooperative networks," *IEEE Transactions on Information Theory*, vol. 56, no. 10, pp. 4981–5000, 2010.
- [41] T. Zhang, A. F. Molisch, Y. Shen, Q. Zhang, H. Feng, and M. Z. Win, "Joint power and bandwidth allocation in wireless cooperative localization networks," *IEEE Transactions on Wireless Communications*, vol. 15, no. 10, pp. 6527–6540, 2016.
- [42] M. Grant and S. Boyd, "CVX users guide for CVX version 1.21 (build 790)," 2010.